DETECTION OF COVID-19 WITH CHEST X-RAY

Ganesh Kumar Yadav[1], Shikhar Singh[2], Shobhit Jain[3],Shivam Shanna[4]

[1]Asst. Professor (Dept. Of CSE), ABES Institute of Technology, Ghaziabad (U.P.)
ganesh.yadav@abesit.edu.in
[2]Computer Science and Engineering, ABES Institute Of Technology, Ghaziabad (UP)
shikhar2018cs015@abesit.edu.in
[3]Computer Science and Engineering, ABES Institute of Technology, Ghaziabad (U.P.)
shobhit201Ses013@abesit.edu.in
[4]Computer Science and Engineering, ABES Institute Of Technology, Ghaziabad (U.p.)
shivam201Scs043@abesit.edu.in

Corresponding Author:

1.ABSTRACT

In order to speed up finding of causes of COVID-19 illness, this study developed novel diagnostic platform using profound convolutional neural network (CNN) helping radiologists diagnose COVID-19 pneumonia beside non-COVID-19 pneumonia in patient in Middle more Hospital. As the name suggests, crucial objective of our research is to produce a chest X-ray image classification program which could properly identify a scan's categorization as either "normal," "viral pneumonia," or "COVID-19." Using X-rays,we will train an image classifier to determine whether or not a person has COVID-19. In this data set, there are over 3000 chest X-ray pictures categorized in normal, viral, as well as COVID-19. A picture classifying system which properly identifies which of three categories Chest X-Ray scan corresponds with is purpose of this investigation.

KEYWORD: *Pneumonia, X-Ray,Covid-19,Convolutional Neural Network*

2. INTRODUCTION

COVID-19 infection may be identified using reverse transcription polymerase chain reaction. Because of worldwide lack of test kits, labs in several countries have been unable to process the tests that are on hand. Health care workers who are seeking to triage patients with symptoms have resorted to chest radiography as an imaging method while efforts to increase RT-PCR testing capability is ongoing.

While many countries struggled to allocate scant sources all through COVID-19 epidemic, underdeveloped countries with infrastructural, economic, healthcare and governmental issues(referred to as "resource-constrained") areparticularly vulnerable. COVID-19 epidemic might pose even much tougher implications in resource-constrained situations than we have previously seen in wealthy countries. According to the WHO, outbreaks had been verified in 45 Africannations as of April 15, resulting in 520 deaths with 10,759 cases. Due to limited accessibility of RT-PCR testing and lack of easy access to medical treatment,

The true numbers are likely to be significantly higher, because of unavailability of RT-PCR assays and the lack of accessibility to medical treatment on A continent. Adequate quarantine and isolation measures must be major part of policy in these locations in order to identify as well as reduce transmission.

To begin with, system was re-trained using a pneumonia data set collected before the COVID-19 pandemic. Despite fact that it has been d-identified, this data is available to anybody who wants it. For currently, there is no information about X-ray systems used to generate it. There are 3000 images in this data set, 7,851 of which are considered to be normal and 5,012 of which are considered to have pneumonia. The other individuals had anomalies that were not compatible with pneumonia.

During the training period, a validation set of 3000 photographs was utilized to assess performance (500/label, consistently splitting through AP and PA pictures). Because it's difficult to get significant numbers of COVID-19 pictures right now, retraining algorithm using this data was a must to improve its sensitivity and specificity for pneumonia in general. Allowing for COVID-19 detection to be optimized. All verified RT-PCR data (except the test set) was included in this data set, along with negative info for balancing class sizes. The technology analyzes a picture in roughly 15 seconds on a typical PC. A picture of highest quality was selected when several CXR images were available for a given subject. Only one image of a child (age 4) was involved in this selection since AI program is projected to communicate with children of this age group and older. A total of 87 images were discarded since these did not displayed whole lung area were either obtained for non-diagnostic reasons such as tube site monitoring. The remaining 468 photos' patient characteristics. More than 2,800 Chest CT are included in this data set, which is broken down to normal, viral pneumonia, and COVID-19. The modules are:

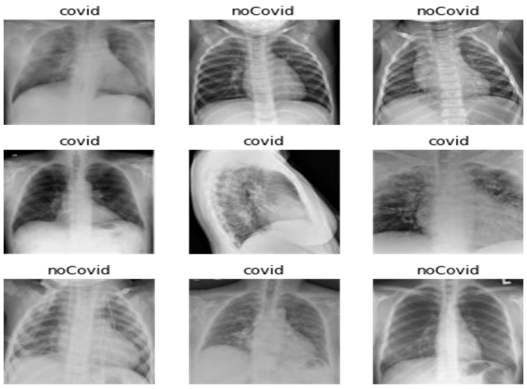

Figure 1 X-ray of COVID and no-COVID Patients

Normal: There was nothing to be found.
Pneumonia like symptoms, but no visible **lung opacity.**
Lung Opacity constant in **pneumonia**
(Implausible COVID-19)

3.RELATED WORK

SARS CoV-2, virus which is a reason for corona virus illness (COVID-19), can only be detected via chest X-ray images, which are crucial both for physician as well as patient in this endeavor. Furthermore, in countries wherein lab kits for tests really are not accessible, this is even more crucial. Purpose of this work was to illustrate how deep learning can be utilized for identifying COVID-19 using chest X-ray pictures having excellent precision. Deep learning as well as machine learning classifiers have been trained on publicly accessible X-ray images as part of the study (4292 pneumonia, 1583 healthy, and 225 verified COVID-19). There were 38 experiments with convolution neural networks, 10 studies involving 5 machine learning models, with 14 investigations with more advanced retrained networks for learning algorithms. As part of the studies, pictures as well as statistical data were analyzed separately to see how well each device performed. The models were tested using an eight-fold

cross-validation procedure. " In terms of sensitivity, overall specificity is 99.18 %, precision value is 98.50 %, as well as average receiver functional features–area under curve scores are 95.51 percent. Convolutional neural networks can identify COVID-19 in a restricted range of unbalanced chest X-ray pictures with few layers but no reprocessing.

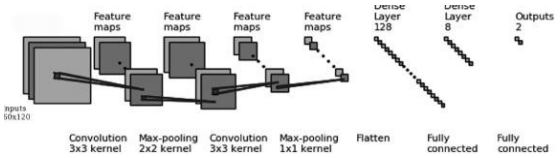

Fig-2 Convolutional neural network1 (ConvNet#1) architecture having 2 convolutional as well as 2 fully connected layers

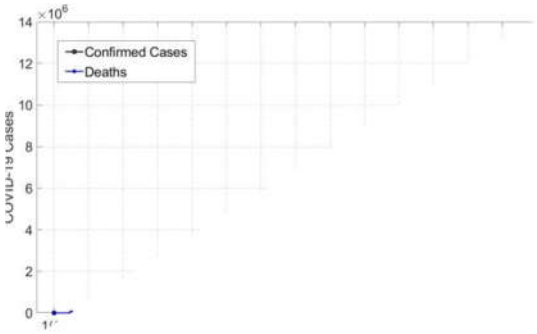

Fig-3 Time-series graph of global total confirmed cases and deaths due to

Time, cost, and accuracy are three most critical aspects in any illness detecting technology, notably COVID-19. COVID-19 occurrences may be detected using CNN-based algorithms proposed in this paper, which addresses these problems. Training is done utilizing 330 chest X-ray pictures, distributed into two classes: "COVID-19" "Normal," which model is developed on. 82 chest X-ray images split evenly are used to verify model.

This model has a 97.56 percent accuracy rate and a 95.34 percent precision rate. In addition, two additional CNN, including one with a varying amount of convolutional layers, are compared against this one. Comparison tests reveal that the suggested model (Model 1) outperforms both the other two (Models 2 and 3). Time, cost, and accuracy are three most critical aspects in either disease detection technology, notably COVID-19. CNN-based approach for categorizing COVID-19 cases from patients' chest X-rays have been proposed into our study to address these difficulties.

Entire 330 chest X-ray pictures have been utilized to train model, which is then separated into two categories: "Normal " and "COVID-19." 82 chest X-ray pictures split evenly are used to verify model.

This model has a 97.56 percent accuracy rate and a 95.34 percent precision rate. A further comparison is made between this model and 2 other CNN models that have differing layers. The suggested model (Model 1) does have better F1-score and performance overall than other two, as shown by comparative analysis.

Figure 4 Sample chest X-Ray images used in model

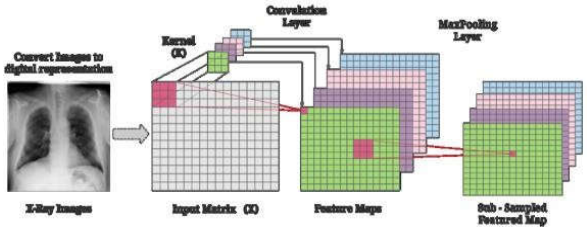

Figure 5 Covid Architecture

The implementation of the HSGO algorithm is discussed in this. It includes setup instructions as well as the various parameters that are utilized into classifiers and algorithm.
The data-set utilized in this study came through "COVID-19 Radiography Record" Kaggle repository.

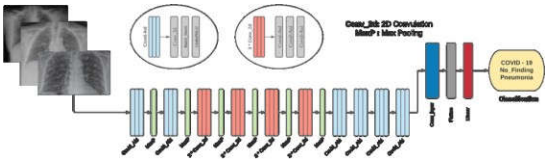

Record of this source included 219 COVID-19 positive shots, 1341 normal pictures, and 1345 viral pneumonia pictures. [31–33]. An additional 152 COVID-19 positive pictures from other comparable causes brought overall quantity of photos for this class up to 371, bringing the final tally to 371.
CXR pictures of COVID-19 positive patients and normal pictures from database have been utilized in our study.
Images of CXRs, the original data set were used to train the final model, which is why this split was made.

4.Materials and Methods

4.1 Dataset

This research employed a minimal dataset of 178 X-ray images as a starting point. There were only 42 photographs of healthy persons or individuals having various diseases in 136 X-rays, whereas the rest of images belonged to COVID-19 patients. There is a GitHub repository where the dataset utilized in this study may be accessible. 136 samples from one COVID-19 class and 42 samples from the other make up the bulk of data set. It was necessary to do preprocessing on an imbalanced dataset in order to get promising findings.
The given original dataset was used to train CNN however, the accuracy was only around 54%, making it unsuitable for present application area. Key data sources utilized in this investigation include the following: A GitHub database of COVID-19 patients' main chest X-ray photos.

University of Montreal's Ethics Committee no. CERSES-20-058-D acquired the data from various clinics as well as hospitals. Images from Kaggle [22] were used to balance out the dataset. (iii) Regarding real-world testing of planned CNN, an experimental validation dataset of 100 COVID-19 X-ray pictures was collected using IEEE Data Port [6].

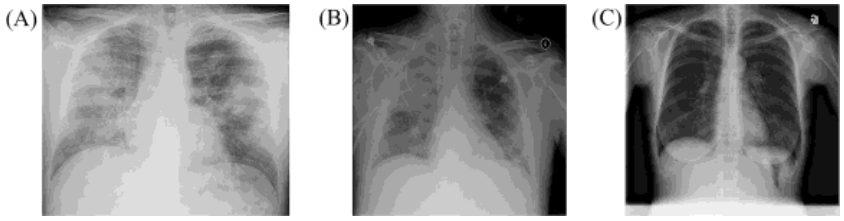

Figure 6 Representative CXR images of COVID-19 pneumonia, non-COVID-19 pneumonia, & healthy. CXR chest X-ray imaging, COVID-19 novel coronavirus disease. (A) COVID-19 pneumonia. (B) Non-COVID-19 pneumonia. (C) No pneumonia

In tests, a 7th generation Core i7 computer having RAM of 8GB, Win-10 was used, as was the Python programming language, along with Anaconda 3, Jupyter Notebook.

1.1 Dataset Preprocessing

1.1.1 Balancing Dataset Classes

For increasing accuracy of proposed CNN models in detecting COVID-19 patients, a dataset of 136 healthy chest X-rays was employed to balance the dataset. The concatenated X-ray picture was download using Kaggle [22]. Following rebalancing dataset and training models once more on created dataset, accuracy of supplied CNN models rose to 69 percent. In spite of this, systems' precision as well as other criteria did not support their usage as an effective method of identifying COVID-19.

1.1.2 Investigation of X-Ray Pictures by Medical Experts

The X-ray images were thoroughly scrutinized by medical professionals. Out of 135 X-ray scans of definite COVID-19 patients, only 90 were picked as excellent candidates for model training. Ninety-nine confirmed COVID-19 reporting and ninety-nine normal X-ray pictures comprised the final sample. The resultant dataset had been utilized for training projected CNN model again, as well as model's performance once again increased. In the case at hand, precision was raised to 72%. Considering this, there's no significant gain in precision or other performance measures because the dataset could not include a significant amount of pictures for successful training.

1.1.3 Data Augmentation

Increasing the quantity of data points in an existing dataset in orders to utilize it in model training is called data augmentation [23]. Using fundamental image processing techniques like flipping, rotating, cropping, and padding to enhance photo datasets, the approach enhances them. [24] The dataset for training neural networks is expanded by including these changed images from the original picture collection. This study used records extension technique to address the issue of a little dataset becoming accessible, that was affecting efficiency of recommended CNN. This method increased dataset size even while giving training model with additional learning properties.

Flipping and rotating images were utilized for records extension in this investigation. A total of 90 new X-ray images were generated in the initial phase of data augmentation. A total of 180 images were generated as a consequence of this method. In the second stage, the original 90 photos have been turned by 90 degrees, then 180 degrees, and finally 270 degrees to produce another 90 photos. A group of 450 COVID-19 X-ray images was generated by following these procedures. Table 2 outlines numerous image processing operations and the number of pictures generated as a consequence of each operation.

Fig. 2 shows original model picture of dataset used in this inquiry before augmentation procedures were applied.

1.2 Convolutional Neural Networks (CNNs)

CNNs were encouraged by visual system of human brain. With CNNs, computers will be able to perceive reality in a similar fashion to how humans do. CNNs may be used to identify and analyze images, classify images, and interpret natural language [25]. CNNs are deep neural networks with convolutional, max pooling, nonlinear activation layers. It is this layer's "convolution" activity that gives CNN its name, and it is regarded a key layer of the network. The kernels of convolutional layer are functional to inputs of layer. CNNs were motivated by human brains visual system. With CNNs, computers will be able to perceive reality in a similar fashion to how humans do. CNNs may be used to identify and analyze images, classify images, and interpret natural language [25]. CNNs are deep neural networks with max pooling, nonlinear activation layers and convolutional. It is this layer's "convolution" activity that gives CNN its name, and it is regarded a key layer of the network. The kernels of convolutional layer are applied to inputs of layer.

CNN relies heavily on pooling layer, often called as sub sampling layer. Each feature map generated by convolution layer is processed individually by pooling layer. In order to diminish over fitting and quantity of extraction of features, it shrinks feature size mapping, returns its chief characteristics. In CNN model, pooling might be sum, the average, or the sum of values. Max pooling has been used in a study since other methods may have a harder time spotting the acute features. Additionally, batch normalization layer was utilized due to fact that this research includes training of very deep neural network.
Modifications in activation and scale are used to normalize and accelerate learning process between hidden units. As an alternative to the over fitting issue, the use of dropout layer, as it is at 20% dropout rate, is being utilized. Output of convolutional layers is transformed in single-dimensional feature vector by a flatting layer at conclusion of the CNN used in the research. With another way of putting it: The flattening layer organizes everything in such a manner that it normalizes input layer and speeds up learning among concealed units. With 20% dropout rate, the dropout layer has been utilized to minimize the over fitting issue by randomly eliminating neurons from training. Convolutional layers' outputs are transformed in single-dimensional

characteristic vector by a flattening layer at the end of the CNN employed in the research. Instead, the flattening layer combines all of convolutional layers' pixels into a single vector for use in the next step in the algorithm. Afterward, it is sent to CNN's next level, known as dense layers or fully linked layers.

An entirely interconnected layer of neurons exists between preceding layer and the one just above it. For the most part, pooling and convolution layers act as input for dense layers, which then use the flattened output results to provide a class label. An attribute's likelihood to fall into a certain category is indicated from every value in the feature set. Thus, the classification decision is made depending upon those probability because of completely connected network with thick layers. 4.3.1.

An RGB 150-by-150 picture is used as the input to proposed CNN model, which has a total of 38 layers: six convolutional (Conv2D), six max pooling (Max Pool), six dropout (Dropout), eight activation function (Activation function), eight batch normalization (Batch Norm), and three fully connected layers. The 3 3 kernel size was utilized in all Con2D levels, however filter size grew with 2 Con2D layers. There were 64 filters utilized for learning through input in the Con2D's first and second levels, 128 filters in 3rd and 4th layers, and a total of 256 filters in 5th and 6th layers.

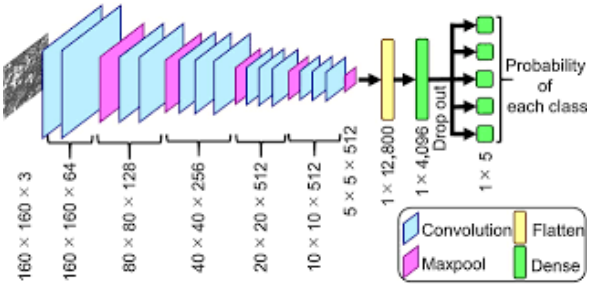

Figure 7 CNN MODEL ARCHITECTURE

The binary cross entropy (BCE) loss function is usedin this work since CNN is used for binaryclassification. Sigmoid activation functions are used because only one output node is required to categorize input into the two predefined classes in binary classification. The activation function of the sigmoid yields value among 0 and 1. It measures the difference between the projected and actual class sizes. Attribute weights and learning rates were changed to reduce the learning model's loss. It is shown in Table 1 and Figure 3 that the model's parameters have been set. During the early experiments, the CNN was used in a variety of configurations, depending on the model's number of convolution layers. Number of convolution layers in model have been determined with use of an incremental method. To begin, CNN has been put to test with just one convolutional layer, as well as outcomes were analyzed. As a consequence, a two-layer CNN had been developed, also results were analyzed and so forth. This technique is being utilized until the model's predictions had been verified. Afterwards, a two-layer CNN was created, and the results were analyzed, and so on. When model's output became efficient and precise, the procedure had been employed for a long time. The final model consisted of six convolution layers and was found to be very feasible based on the findings. Each model increment's outcomes are summarized in the Outcomes section.

4.4 Deep learning model and data augmentation.

Using VGG16 as a deep learning model, transfer learning was utilized to categorize COVID-19, non-COVID-19 pneumonia, healthy CXRs. Our first results show that VGG16 overfits and worsens performance when it lacks transfer learning. For VGG16-based model and data augmentation approaches, random search was employed to determine the optimal hyperparameters. A deep learning model is shown in Figure 1.
Using pre-trained models on the ImageNet dataset, we were able to create our own VGG16 weights for transfer learning. First to tenth layers of VGG16 was froze after transfer learning, as well as layers of VGG16 was arranged in order in which they were processed in original image.

Category	Value
Number of images	1248
Sex	
Male	512
Female	702
Not available	34
Age	
Available	1205
Not available	43

Models	Loss of test set	3-category accuracy of test set (%)
VGG16 (proposed method)	0.4682 ± 0.0289	83.68 ± 2.00
Resnet-50	0.5237 ± 0.0161	77.76 ± 1.18
MobileNet	0.4919 ± 0.0300	78.72 ± 3.22
DenseNet-121	0.5276 ± 0.0082	78.24 ± 2.23
EfficientNet	0.5206 ± 0.0177	78.40 ± 1.82

		Prediction by the proposed model		
		The healthy	Non-COVID-19 pneumonia	COVID-19 pneumonia
Ground truth	The healthy	43	7	0
	Non-COVID-19 pneumonia	9	41	3
	COVID-19 pneumonia	2	0	20

Mean ± SD of age (years)	48.1 ± 17.5
Diagnosis	
COVID-19	215
Non-COVID-19 pneumonia	533
The healthy	500
CXR view	
PA	666
AP	582

Table 1. Characteristics of patients and CXR qualities COVID-19 new coronavirus illness, SD standard deviation, PA posterior–anterior view, AP anterior–posterior view, CXR chest X-ray imaging

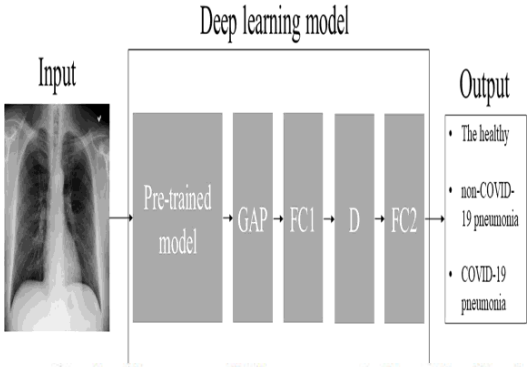

Figure 8. A diagram of the suggested method's deep learning model. VGG16, Resnet-50, MobileNet, DenseNet-121, and EfficientNet were employed in the current investigation for pre-trained models. For the sake of brevity, the activation function has been omitted. Global averaging pooling layer (GAP), FC fully-connected layer (FC), and D dropout layer (D dropout layer).

After convolution layers, global average pooling layer, the fully connected layer, and the dropout layer have been added. Last three-unit fully connected layer were added for three-category classification after the dropout layer was implemented. Correction of a linear unit as well as SoftMax were used as activation functions in the first and final completely linked layers. VGG16-based model random search revealed these hyperparameters. There were 416 units in the first fully linked layer, and the dropout probability was 0.1. By optimizing the learnable parameters of VGG16's non-frozen layers including totally linked layers, RMSprop reduced cross - entropy loss among class labels and model outputs by 1.0 10–4.
It was changed into 220 x 220 pixels for VGG16's input picture to fit on screen. A total of eight batches and 100 training epochs were used to train network. When validation errors occurred, it was possible to stop the experiment sooner rather than later.

Table 2. 5 models that have already been trained. Mean standard deviation for ±5 trials was used to get the value of each cell.

Table 3. The test set's 3-category categorization confusion matrix. Accuracy was 83.2% (104/125).

6.Comparison with other pre-trained models and ablation study.

For associating by VGG16-based model, 4 pre-models have been utilized for allocation learning: MobileNet, Resnet-50, Efficient Net and DenseNet-121. In transfer learning using these 4 pre models, learnable factors were not frozen; freezing learnable parameters in such models reduced model performance. Random searches for idealhyperparameters and combinations of dataaugmentation approaches were also conducted forfour pre-trained models. The best model for EfficientNet was chosen by random search from B0–B7.
The subsequent updated models also were examined for VGG16-based model for evaluating efficiency of data augmentation techniques as well as freeze of trainable parameters: I have no data augmentation with freezing, (ii) conventional technique just with freezing, (iii) mix-up solely with freezing, and (iv) conventional technique, mix-up without freezing.

Models	Loss of test set	3-category accuracy of testset (%)
proposed Method	0.462 ± 0.029	83.635± 2
No data augmentation with layer freezing	0.909 ± 0.1967	78.71 ± 1.66
Conventional \data augmentation	0.483 ± 0.0274	82.46 ± 2.46
mix- up only with\ layer freezing	0.6407 ± 0.0674	79.2 ± 1.74
conventional data augmentation method and mixup without layer freezing.	0.513 ± 0.019	79 ± 2.6

Table 4. The ablation research of projected approachfor data augmentation methods as well as layer freezing produced the following results. Each cell's value was themean minus the standard deviation of five trials.

7. Results

Table 2 displays results of the proposed method's three classifying of COVID-19 pneumonia, no-COVID-19 pneumonia, as well as normal for five pre-trained models. The researchers employed a mix of data augmentation approaches and a random search to determine the optimum hyperparameters. Training time per epoch were lower than 20 seconds in top VGG16-based model. The recommended method's VGG16-based model has an 83.7 percent mean accuracy, as shown in Table 2. MobileNet, Resnet-50, EfficientNet and DenseNet-121. all exhibit lower mean accuracies than the proposed approach's VGG16-based model, with mean accuracies of less than 80%. VGG16-based model provides a 90.9 percent mean sensitivity for COVID-19 pneumonia. Table 3 in the test set shows a sample confusion matrix of three-category categorization.

Table 4 investigated efficacy of data augmentation options as well as freezing of trainable bounds in VGG16-based model. Table4 depicts as layer freezing worked successful. Because it incorporated two forms of data augmentation techniques, the suggested approach proved higher efficient than a single kind or no data preprocessing methods.
The results of random search for RICAP are provided in additional information. Because random search results outperformed other methods examined (standard technique, mix-up, and RICAP), it was decided to use random search results instead. In comparison to traditional technique and mixup combo, traditional method and RICAP approach fared somewhat worse. Thus, present research did not thoroughly investigate combinationof traditional methods withRICAP.

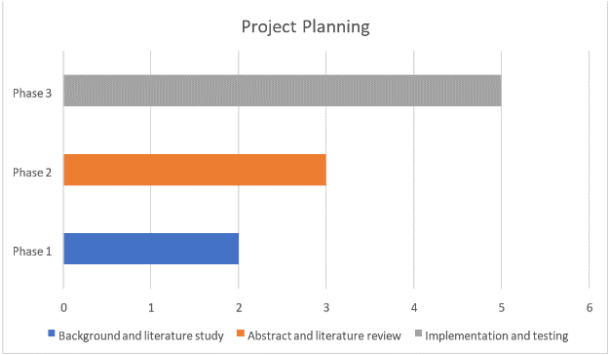

8. Discussion

Findings of this study show that an accurate CNN model can be developed using such learning algorithm of VGG16 and a variety of data enhancement techniques. The clinical diagnosis of the proposed method for the 3 extended classifications among non-COVID-19 pneumonia, COVID-19 pneumonia, normal was greater than 81%, according to our findings. COVID-19 is also highly sensitive, with a sensitivity of over 92%.
Utilizing two types of data enhancement was more beneficial than utilizing just one type of data enhancement approach or nothing at all, as shown in Table 4. Our findings matched those from a prior CNN15-based bone segmentation study. The resilience of CNN models had to be improvedbecause the current study's dataset was rather short(only 1248 CXR pictures). To attain this goal, present research utilized a mix of data augmentation methodologies. A mixture of traditional and mix-uptactics proved to be the most effective strategy.
VGG16 was the most accurate of the various kinds of pre-trained models for the 3-category classification. Our results did not equal the ImageNet dataset's classification accuracy, despite the fact that the ImageNet dataset's classification accuracy was greater in other models than in VGG16.

Other models (such as residue learning) or their integration of a great amount of trainable parameters may have overfitted owing to the small dataset in the present research. As a result of the large number of learnable parameters and the complicated network topology, hyperparameter tweaking was more challenging into DenseNet-121, Resnet, MobileNet, and EfficientNet than in VGG16.
Utility of pre-trained models should be examined further in a limited dataset.The layers hardening of the training data was only effective in VGG16. VGG16's network design is less complex than those of its predecessors. Layer freezing may be hampered if connections are skipped for residual connections in the other network. The utility of layers cooling in CNN models may be compromised as a result of this. Several previous studies linked CXR photos of no-COVID-19 pneumonia with mature CXR pictures of COVID-19 pneumonia to construct databases, per an article from towarddatascience.com.

To train a CNN model, these datasets may be utilized to look at age gaps amongst adults and children, rather than illness differences, in demand to recognize non-COVID-19 and COVID-19 pneumonia. As a result, this study solely employed adult CXR images from the RSNA dataset of healthy and non-COVID-19 pneumonia patients. Our research has a few drawbacks. First, we usedavailable datasets to build and validate thesuggested technique. The current study's findingsmerely illustrate that our CADx technology iscapable of excellent accuracy in public datasets.Public datasets may have characteristics that differ from clinical data. Overfitting may have occurredduring external validation in this scenario. Clinicaldata will be used to investigate the utility of CADx technology. Second, CADx system was not used by clinicians. The CADx technology's clinical value has yet to be determined.

9. CONCLUSION

Finally, the proposed method can be used to develop an accurate CADx system for non-COVID-19 pneumonia, COVID-19 pneumonia, also with healthy. With two types of data augmentation strategies instead of just one or none at all proven to be more beneficial. Whereas clinical CXR pictures of non-COVID-19 pneumonia, COVID-19 pneumonia, and healthy patients were served into our CADx system, we'll see how well it worked.

10. REFERENCES

[1] W. Yang, A. Sirajuddin, X. Zhang, G. Liu, Z. Teng, S. Zhao, M. Lu, "The role of imaging in 2019novel coronavirus pneumonia (COVID- 19)," European Radiology, vol. April 15, pp. 1- 9, 2020.

[2] G. D. Rubin, C. J. Ryerson, L. B. Haramati, N. Sverzellati, J. P. Kanne, S. Raoof, N. W. Schluger, A. Volpi, J.-J. Yim, I. B. K. Martin, D. J. Anderson, C. Kong, T. Altes, A. Bush et al, "TheRole of Chest Imaging in Patient Management during the COVID-19 Pandemic: A Multinational Consensus Statement from the Fleischner Society," Radiology, vol. Apr 7, 2020.

[3] M. P. Cheng, J. Papenburg, M. Desjardins, S. Kanjila, C. Quach, M. Libman, S. Dittrich, C. P. Yansouni, "Diagnostic Testing for Severe AcuteRespiratory Syndrome–Related Coronavirus-2: ANarrative Review," Annals of Internal Medicine, vol. 13 Apr, 2020.

[4] Jacobi, M. Chung, A. Bernheim, C. Eber, "Portable chest X-ray in coronavirus disease-19 (COVID-19): A pictorial review," Clinical Imaging, vol.64,pp.35-42, 2020. Crossref, Medline.

[5] World Health Organisation, situation reports on COVID-19 outbreak," 15 April 2020. [Online]. Available: https://apps.who.int/iris/bitstream/handl e/10665/331763/SITREP_COVID- 19_WHOAFRO_20200415-eng.pdf.

[6] D. J. Mollura, P. M. Lungren, Radiology in Global Health, Strategies, Implementation, and Applications, Springer, 2019. Crossref,

[7] E. J. Hwang, J. G. Nam, W. H. Lim, S. J. Park, Y.S. Jeong, J. H. Kang, E. K. Hong, T. M. Kim, J. M. Goo, S. Park, K. H. Kim, C. M. Park, "DeepLearning for Chest Radiography Diagnosis in theEmergency Department," Radiology, vol. 293, no. 3, 2019.

[8] M. Annarumma, S. J. Withey, R. J. Bakewell, E. Pesce, V. Goh, G. Montana, "Automated Triaging of Adult Chest Radiographs with Deep Artificial Neural Networks," Radiology, vol. 291, no. 1, 2019.

[9] K. Murphy, S. S. Habib, S. M. A. Zaidi, S. Khowaja, A. Khan, J. Melendez, E. T. Scholten, F. Amad, S. Schalekamp, M. Verhagen, R. H. H. M. Philipsen, A. Meijers, B. v. Ginneken, "Computer aided detection of tuberculosis on chest radiographs:An evaluation of the CAD4TB v6 system," Scientific Reports, vol. 10, 2020.

[10] Z. Z. Qin, M. S. Sander, B. Rai, C. N. Titahong, S. Sudrungrot, S. N. Laah, L. M. Adhikari, E. J. Carter, L. Puri, A. J. Codlin, J.Creswell, "Using artificial intelligence to read chestradiographs for tuberculosis detection: A multi-site evaluation of the diagnostic accuracy of three deep learning systems," Scientific Reports, vol. 9, 2019.